

HADRONIC JETS FROM e^+e^- -ANNIHILATIONS IN THE Υ - AND Υ' -REGION[☆]

DESY—Hamburg—Heidelberg—MPI München Collaboration

F.H. HEIMLICH, P. LEZOCH and U. STROHBUSCH

I. Institut für Experimentalphysik, Hamburg, Germany

P. BOCK, G. HEINZELMANN and B. PIETRZYK

Physikalisches Institut der Universität, Heidelberg, Germany

G. BLANAR, W. BLUM, H. DIETL, E. LORENZ and R. RICHTER

Max-Planck-Institut für Physik, München, Germany

J.K. BIENLEIN, M. LEISSNER, E. METZ, B. NICZYPORUK¹,

C. RIPPICH, M. SCHMITZ and H. VOGEL²

DESY, Hamburg, Germany

Received 17 July 1979

Electron–positron annihilations into hadrons were observed in the region of the Υ (9.46 GeV) and the Υ' (10.02 GeV) resonances at the storage ring DORIS with the nonmagnetic NaI lead–glass detector. Distributions of sphericity and charged multiplicity were measured. Outside the resonances the data show a clear two-jet structure, while the decays of the resonances are compatible with the predictions of a three-gluon model.

In recent experiments [1–3], the Υ (9.46) and Υ' (10.02) resonances were observed in e^+e^- -annihilations into hadrons at the upgraded storage ring DORIS [4]. These resonances are interpreted as bound states of a quark–antiquark pair with $J^{PC} = 1^{--}$. In the framework of quantum chromodynamics, they should mainly decay via three gluons [5] which in turn fragment into hadrons. Therefore, a more isotropic particle distribution and possibly a three-jet structure is expected in contrast to the continuum where a two-jet structure has been observed [6,7a]. In addition, depending on the fragmentation of quarks and gluons into

hadrons, a change in multiplicity is expected for the Υ and Υ' decays as compared to the continuum.

In the present paper, we analyze the hadronic events obtained during Υ , Υ' and continuum studies [3] in terms of sphericity and thrust. As a particular feature of this experiment, these variables were determined primarily from hadrons decaying into photons. A similar study has been done by the PLUTO collaboration in the Υ region and in the continuum [7] mainly using the charged fraction of the events. In addition, we present multiplicity distributions for charged particles.

The hadronic events were observed with the non-magnetic DESY–Heidelberg detector described in several publications [8]. The inner detector consisted of three cylindrical double drift chambers which measured the direction of charged tracks and two scintillation hodoscopes for triggering purposes. It was surrounded by an outer detector consisting of NaI and

[☆] Work supported by the Bundesministerium für Forschung und Technologie.

¹ On leave from: Institute of Nuclear Physics, Cracow, Poland.

² On leave from: Physikalisches Inst. der Universität, Erlangen, Germany.

lead-glass blocks which measured the energy of electromagnetic showers. The energy resolution of the shower counters was approximately $12\%/\sqrt{E}$, where E is expressed in GeV. Coordinates of showers were measured from the position of shower counters and the energy sharing between them or from conversion points measured in the drift chambers. The photon direction was measured with a precision varying between 30 and 200 mrad. In general, minimum ionizing particles deposited an energy of about 200 MeV in the shower counters. The detector covered 86% of 4π .

A very loose on-line trigger, requiring at least one charged track in the inner detector and more than 250 MeV deposited in the apparatus, was used to detect e^+e^- annihilations into hadrons. In order to remove background from beam-gas interactions, cosmic rays and QED processes, the off-line selection for hadrons required three or more charged tracks and at least 1.8 GeV total measured energy. In addition, more than 5% of the total observed energy had to appear in any half of the detector and at least 10% of the energy had to be correlated with charged tracks. Final selection was done by a hand scan thus eliminating misinterpreted Bhabha scattering events. The reconstructed interaction vertex peaked well in the region of e^+e^- bunch crossing. From the vertex distribution, the background from beam-gas interactions and cosmic ray events was estimated to be 2.5% inside the accepted interaction region of ± 30 mm. About 10% of the continuum events were estimated to be due to the hadronic decays of the heavy lepton τ . The total efficiency for detecting hadronic events was of the order of 90%. The number of hadronic events obtained is shown in table

1 together with the luminosities and energy ranges. The number of events from the direct decay of the Υ into hadrons as given in table 1 was obtained by subtracting the nonresonating continuum part under the resonance and the Υ -decay via one virtual photon. The small contribution of the virtual photon decay was determined using results for $e^+e^- \rightarrow \mu\mu$ on and off-resonance from ref. [7b].

In order to study the spatial momentum distribution, we used the global variables sphericity S and thrust T defined as:

$$S = (3/2) \min \left(\sum_i p_i^{\perp 2} \right) / \sum_i p_i^2,$$

and

$$T = \max \sum_i |p_i^{\parallel}| / \sum_i |p_i|,$$

Σ_i = sum over all particles of an event, p_i^{\perp} = transverse momentum component, p_i^{\parallel} = longitudinal momentum component and p_i = total particle momentum. S and T are calculated with respect to the sphericity and thrust axes. The sphericity axis is obtained by minimizing the sum of squared momenta transverse to it, the thrust axis by maximizing the sum of momenta parallel to it. For the extreme case of a pure two-jet event, one expects $S \rightarrow 0$ and $T \rightarrow 1$ while for an ideal spherical event (isotropic angular distribution) one would find $S \rightarrow 1$ and $T \rightarrow 1/2$.

In our analysis, the momenta in the above definitions were replaced by the momenta $\mathbf{p} = E \cdot \mathbf{e}$, using the measured energies (E) and their positions (unit vector \mathbf{e}) in the detector. The summation was done

Table 1
Luminosities, energy ranges and numbers of hadronic events in the Υ and the Υ' region.

	Υ region	Υ' region
integrated luminosity	173 nb ⁻¹	120 nb ⁻¹
energy range of continuum	9.41–9.44 GeV 9.48–9.52 GeV	9.98–10.00 GeV 10.04–10.10 GeV
events of continuum	327	165
energy range "ON" resonance	9.455–9.460 GeV	10.014–10.028 GeV
events "ON" resonance	695	181
events from direct resonance decay	≈427	≈70

over all observed energies. Since charged tracks contribute generally only about 200 MeV, the sphericity and thrust values measured with our apparatus are primarily sensitive to the neutral fraction of events, i.e. to π^0 's and η 's decaying into photons. This same procedure was also applied to events generated by a Monte-Carlo method. It is shown later that the sphericity values obtained with this procedure are useful for testing various production processes, in particular the two-jet and three-jet decay modes. The real quantities S , T and charged multiplicity, unaffected by the detector, can be deduced if we assume a specific model. Since the measured difference between the thrust axis and the sphericity axis is approximately 15° (FWHM) and the measured thrust follows the relation $T \approx 1 - 0.5 \cdot S$ with $\Delta T \approx \pm 0.05$, we will concentrate in the following mainly on distributions of sphericity.

Fig. 1a shows the experimental distribution of our sphericity from cms energies below and above the Υ resonance. The distribution peaks strongly at small S as expected for e^+e^- -annihilation into two jets. The solid line is a Monte-Carlo calculation using the production of a quark-antiquark pair by a virtual photon and a standard fragmentation into mesons following the parametrization of Field and Feynman [9]. The Monte-Carlo calculation included radiative corrections, detector acceptance, event selection criteria and the reconstruction procedure. It also simulated the energy

deposition of neutral and charged particles including possible hadronic interactions. Contributions from charmed mesons and heavy leptons are not included in this calculation. The observed sphericity distribution as well as the mean sphericity of 0.227 ± 0.010 (given in table 2a) are well reproduced by this Monte-Carlo calculation. The two-jet model yields a real mean sphericity, unaffected by the detector, of 0.231 ± 0.003 (table 2b).

Fig. 1b shows the experimental sphericity distributions for events in the Υ resonance after bin by bin subtraction of the expected contribution from the continuum and from virtual photon decay of the resonance. This procedure has also been applied for the subsequent distributions of direct Υ decays. From the figure we can see that the maximum of the sphericity distribution is shifted to higher sphericity values with respect to the off-resonance distribution, indicating a substantial change in event shape towards more spherical decays. The solid line is a Monte-Carlo prediction for the decay of the Υ into three gluons. In this calculation, we used the QCD-matrix element [10] and assumed that the gluons fragment exactly like quarks with the same momentum. This three-gluon decay prediction describes the data very well both in the mean value and shape of the distribution. Also shown in fig. 1b as a dashed line is the expected distribution for an assumed decay of the Υ into pions according to phase

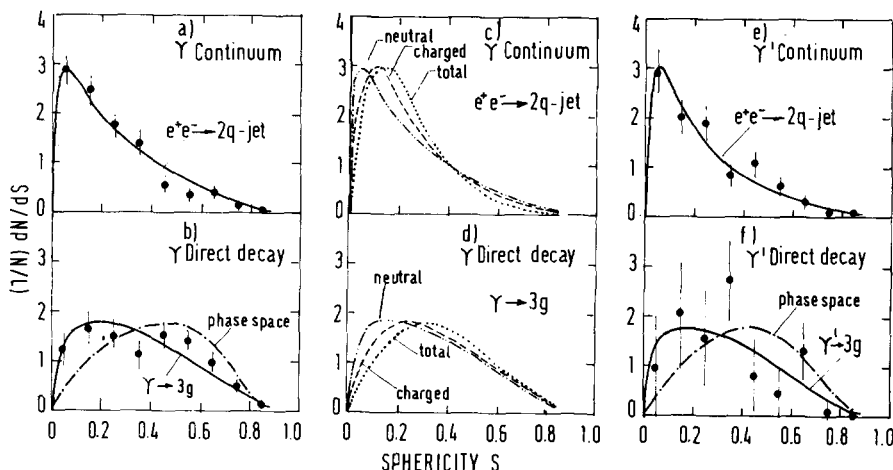


Fig. 1. Differential sphericity distributions for $e^+e^- \rightarrow$ hadrons. (ab) Experimental sphericity distributions for the Υ region compared to Monte-Carlo calculations including detector corrections. See text for details of the two-quark-jet, three-gluon decay and multi-pion phase space models shown. (cd) Model predictions without detector corrections showing the distribution for complete events as well as for the neutral and charged fractions. (ef) Distributions for the Υ' region as in (ab).

Table 2

Mean values for the sphericity S , thrust T and charged multiplicity n_{ch} for the Υ and Υ' region. All quoted errors are purely statistical.

		MC 2-quark	Experiment		MC	
			off	direct	3-gluon	phase space
Experimental and Monte-Carlo values including detector corrections ^{a)}						
Υ	$\langle S \rangle$	0.243 ± 0.005	0.227 ± 0.010	0.365 ± 0.014	0.332 ± 0.006	0.427 ± 0.006
	$\langle T \rangle$	0.801 ± 0.003	0.819 ± 0.005	0.736 ± 0.007	0.753 ± 0.003	0.713 ± 0.003
	$\langle n_{\text{ch}} \rangle$	6.2 ± 0.1	6.1 ± 0.2	6.9 ± 0.2	6.8 ± 0.1	6.8 ± 0.1
Υ'	$\langle S \rangle$	0.232 ± 0.005	0.247 ± 0.016	0.316 ± 0.044	0.325 ± 0.006	0.414 ± 0.006
	$\langle T \rangle$	0.805 ± 0.003	0.813 ± 0.008	0.767 ± 0.022	0.754 ± 0.003	0.716 ± 0.003
	$\langle n_{\text{ch}} \rangle$	6.3 ± 0.1	5.9 ± 0.2	7.5 ± 0.6	7.0 ± 0.1	7.0 ± 0.1
Monte-Carlo values without detector corrections ^{b)}						
Υ	$\langle S \rangle_{\text{total}}$	0.231 ± 0.003			0.391 ± 0.005	0.579 ± 0.005
	$\langle S \rangle_{\text{neutral}}$	0.235 ± 0.004			0.323 ± 0.006	0.377 ± 0.007
	$\langle S \rangle_{\text{charged}}$	0.234 ± 0.004			0.354 ± 0.005	0.511 ± 0.006
	$\langle n_{\text{ch}} \rangle$	7.7 ± 0.1			8.4 ± 0.1	8.6 (fixed)

a) The experimentally observed values are to be compared with the two-quark, three-gluon and phase space calculations on the same line, which include radiative corrections, detector acceptance and the analyzing method.

b) For the Υ region, the real values, unaffected by the apparatus, are listed.

space, which is the limiting case of an isotropic decay. Here, we assumed the multiplicity distribution to be Poisson-like with $\langle n_{\text{charged}} \rangle = 8.6$ and $\langle n_{\text{neutral}} \rangle = 4.3$ to reproduce the observed multiplicities. This multipion phase space model differs from the data predicting higher sphericity values.

In order to demonstrate the relation between the real sphericity and the expected experimental one, Monte-Carlo studies for the two-jet and three-gluon decay model are shown in figs. 1c and 1d. The distributions for complete events as well as their charged and neutral fractions have been calculated using the momenta of particles generated by the Monte-Carlo

program without detector corrections. These curves have to be compared with the expected experimental distributions (solid lines) in figs. 1a and 1b, which have been obtained by generating the energy deposition of photons and charged hadrons in the detector and applying the pattern recognition program and analyzing methods also used for the data. One can see that the distributions for the neutral fraction of the events, unaffected by the detector, in figs. 1c and 1d are very similar to the predicted experimental ones in figs. 1a and 1b. By comparing the curves in figs. 1a and 1b one concludes furthermore that the predicted experimental distribution is a good way to distinguish be-

tween different models such as two-quark and three-gluon assumptions.

The observed sphericity distribution for the continuum events around the Υ' in fig. 1e shows the same shape as the continuum around the Υ . The two-quark model (solid line) fits the data well. Fig. 1f shows the distribution for the direct decay of Υ' . One cannot discriminate between different models because of low statistics.

Fig. 2a and 2b show the angular distributions of the sphericity axis with respect to the e^+e^- -beam for the continuum and the Υ resonance, respectively. To improve the statistical significance, data from the continuum around the Υ and Υ' have been combined. For the continuum, we omitted events with sphericities greater than 0.5 because of the poor definition of the axis. The acceptance of the apparatus was essentially 100% for $\cos \theta < 0.6$. A fit of $1 + \alpha \cos^2 \theta$ in the range $0 \leq |\cos \theta| \leq 0.6$ yields $\alpha = 1.5 \pm 0.6$. This is in agreement with the expectation of $\alpha = 1$ for a virtual photon coupling to two spin 1/2 quarks. In fig. 2b the angular distribution is shown for the direct decays of the Υ . The distribution is flatter, the fit result of $\alpha = -0.1 \pm 0.8$ is consistent with a three-gluon predic-

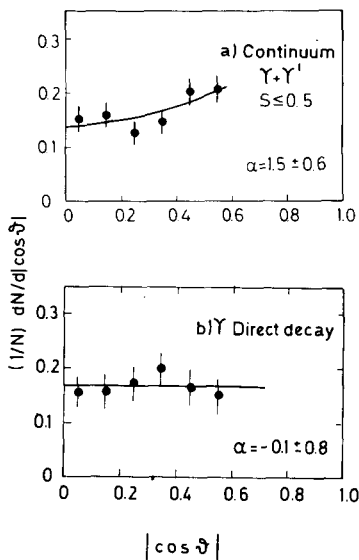


Fig. 2. Angular distributions of the sphericity axis. θ is the angle between sphericity and beam axes. The solid line shows $dN/d|\cos \theta| \approx 1 + \alpha \cos^2 \theta$. (a) Continuum around Υ and Υ' , events with sphericities ≤ 0.5 are shown. (b) Direct decay of the Υ .

tion of $\langle \alpha \rangle = 0.39$ [10] for the thrust axis.

The multiplicity of particles in the final states was studied to gain insight into gluon fragmentation. In this experiment the number of charged tracks including beam-pipe conversions have been determined by counting the straight tracks seen in the polar projections of the cylindrical drift chambers. Fig. 3a shows the observed charged multiplicity for the events from the continuum around the Υ resonance. The broken curve indicates the real charged multiplicity as generated by a Monte-Carlo calculation following the standard model of Field and Feynman for two-jet events. The solid curve is this same distribution after radiative corrections, acceptance cuts for the apparatus and beam-pipe conversions. The data are well described by this curve. The prediction of a mean multiplicity of 7.7 ± 0.1 from the two-jet model implies an observed multiplicity of 6.2 ± 0.1 after our acceptance cuts. We find a multiplicity of 6.1 ± 0.5 , which is in complete agreement. The error in the measured data is dominated by a systematic contribution of ± 0.5 units due to pattern recognition problems. This systematic error is common

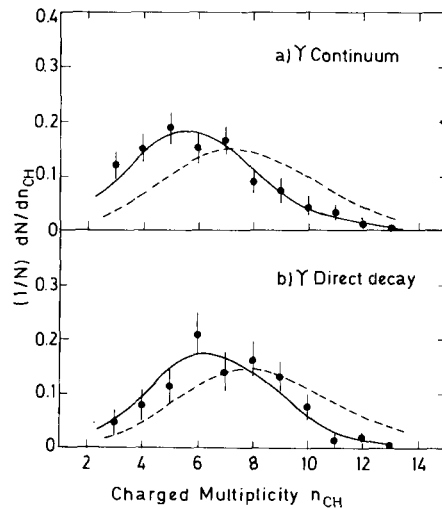


Fig. 3. Distributions of the observed multiplicity of charged particles including beam-pipe conversions. (a) Continuum around the Υ . The solid line shows the two-quark-jet Monte-Carlo calculation including detector corrections, while the dashed line indicates the multiplicity distribution without detector corrections and beam-pipe conversions. (b) Direct decay of the Υ . The solid line shows the three-gluon Monte-Carlo calculation including detector corrections, while the dashed line indicates the multiplicity distribution without detector corrections and beam-pipe conversions.

to all multiplicity values. For the continuum region around the Υ' resonance, approximately the same value has been observed (table 2).

For the direct Υ decays, the observed charged multiplicity distributions is shown in fig. 3b. An increase of (0.8 ± 0.2) in the mean multiplicity compared to the continuum is observed. For multiplicity changes the systematic contributions to the errors cancel and only the statistical error apply. Assuming that gluons fragment like quarks with the same momentum and adopting the QCD prediction of the Υ decay via three gluons, we can predict the charged multiplicity distribution. The broken curve in the figure indicates the real charged multiplicity as generated by the three-gluon Monte-Carlo calculation while the solid curve gives the multiplicity of tracks from charged particles and beam-pipe conversions after experimental cuts. For the direct Υ' decays, an increase in the mean multiplicity of (1.6 ± 0.7) compared to the continuum is observed.

In summary, two-jets structure has been observed for e^+e^- -annihilations into hadrons in the continuum around the $\Upsilon(9.46)$ and $\Upsilon'(10.02)$ resonances. The angular distribution of the jet axis is compatible with $1 + \cos^2\theta$ as expected from the quark parton picture. The observed sphericity and charged multiplicity can be well described by a two-jet model with a quark fragmentation according to Field and Feynman.

For the direct decays of the Υ and Υ' resonances, we observe an increase in sphericity and charged multiplicity as compared to the continuum. The observed distributions for the sphericity and charged multiplicity

are in good agreement with the assumption that the Υ resonance decays mainly via three gluons which in turn fragment into hadrons like quarks with the same momentum, although a phase space-like decay cannot be completely excluded.

We would like to thank DESY for the excellent support given to the experiment. We are also grateful to the old DESY-Heidelberg group for the use of their detector and software and H.J. Meyer from the PLUTO collaboration for providing us with the thrust computer program.

References

- [1] Ch. Berger et al., PLUTO Collaboration, Phys. Lett. 76B (1978) 243.
- [2] C.W. Darden et al., DASP II Collaboration, Phys. Lett. 76B (1978) 246; 78B (1978) 364.
- [3] J.K. Bienlein et al., DESY-Hamburg-Heidelberg-MPI München Collaboration, Phys. Lett. 78B (1978) 360.
- [4] W. Bothe et al., DORIS storage ring group, DESY Report 79/08 (1979).
- [5] T. Appelquist and H.D. Politzer, Phys. Rev. D12 (1975) 1404.
- [6] G. Hanson et al., Phys. Rev. Lett. 35 (1975) 1609.
- [7] Ch. Berger et al., PLUTO Collaboration, (a) Phys. Lett. 78B (1978) 176; (b) 82B (1979) 449; (c) 81B (1979) 410.
- [8] W. Bartel et al., Phys. Lett. 64B (1976) 483; 77B (1978) 331.
- [9] R.D. Field and R.P. Feynman, Nucl. Phys. B136 (1978) 1.
- [10] K. Koller, H. Krasemann and T.F. Walsh, Z. Phys. C1 (1979) 71.